*Metallophysics and Advanced Technologies*
*Металофіз. новітні технол.*
*Metallofiz. Noveishie Tekhnol.*
2025, vol. 47, No. 10, pp. 1043–1059
https://doi.org/10.15407/mfint.47.10.1043
Reprints available directly from the publisher



PACS numbers: 43.35.Zc, 43.40.Le, 68.35.Iv, 68.60.Bs, 68.65.Ac, 81.15.-z, 81.70.Cv

# Research on the Properties of Multilayer Nitride CrN/NbN Coatings Using Acoustic Emission Parameters. Pt. 2. Multilayer CrN/NbN Coatings with Bilayer Thickness of 67 nm

I. V. Serdyuk[*], S. I. Petrushenko[**,***], V. O. Stolbovyy[*,****], and M. Fialkowsky[***]

[*]*National Science Centre*
*'Kharkov Institute of Physics and Technology', N.A.S. of Ukraine,*
*1 Akademichna Str.,*
*UA-61108 Kharkiv, Ukraine*
[**]*V. N. Karazin Kharkiv National University,*
*4 Svobody Sqr.,*
*UA-61022 Kharkiv, Ukraine*
[***]*Technical University of Liberec,*
*Studentska 1402/2,*
*46117 Liberec 1, Czech Republic*
[****]*Kharkiv National Automobile and Highway University,*
*25 Yaroslava Mudrogo Str.,*
*UA-61002 Kharkiv, Ukraine*

The investigation of the properties of the vacuum-arc multilayer nitride CrN/NbN coatings with 270 layers and bilayer thickness of 67 nm is performed using a method of acoustic emission. The investigation is conducted using scratch testing and microscopic visual observation of scratches. Methods for statistical data analysis of acoustic emission are applied for comparing the properties of multilayer CrN/NbN coatings obtained at different technological parameters of deposition (the constant negative voltage on the

Corresponding author: Iryna Vitaliyivna Serdyuk
E-mail: iraserduk@kipt.kharkov.ua

Citation: I. V. Serdyuk, S. I. Petrushenko, V. O. Stolbovyy, and M. Fialkowsky, Research on the Properties of Multilayer Nitride CrN/NbN Coatings Using Acoustic Emission Parameters. Pt. 2. Multilayer CrN/NbN Coatings with Bilayer Thickness of 67 nm, *Metallofiz. Noveishie Tekhnol.*, **47**, No. 10: 1043–1059 (2025). DOI: 10.15407/mfint.47.10.1043

substrate of 70–200 V and the nitrogen pressure in vacuum chamber of 0.08–0.27 Pa). Several parameters of acoustic emission (the maximum pulse amplitude, the average value, the median value, the mode value, the number of pulses, and the amplitude sum of all acoustic-emission pulses) are calculated for each coating. The studied parameters are calculated on four scratches for each multilayer coating. The influence of deposition technological parameters on the structure deformation processes of multilayer CrN/NbN coatings with 270 layers and bilayer thickness of 67 nm occurred during scratch testing is determined.

**Key words:** multilayer coatings, cathodic arc evaporation, acoustic emission, deformation, methods for statistical data analysis, coating embrittlement.

Дослідження властивостей вакуумно-дугових багатошарових нітридних CrN/NbN-покриттів, що складаються з 270 шарів із товщиною бішару у 67 нм, було проведено із використанням параметрів акустичної емісії. Дослідження проводилися під час скретч-тестування за рахунок оцінювання параметрів акустичної емісії та візуального обстеження подряпин за допомогою мікроскопії. Для порівняння властивостей багатошарових CrN/NbN-покриттів, одержаних за різних технологічних параметрів осадження (за постійної неґативної напруги на підкладинці у –70–-200 В, тиску азоту у вакуумній камері у 0,08–0,27 Па), було застосовано методи статистичної аналізи випадкової величини акустичної емісії. Для кожного багатошарового покриття було визначено максимальну амплітуду імпульсу, середнє значення, медіяну, моду, кількість імпульсів і суму амплітуд усіх імпульсів. Досліджувані параметри оцінювалися по чотирьох подряпинах для кожного багатошарового покриття. Встановлено вплив технологічних параметрів осадження на деформаційні процеси, що відбуваються в структурі багатошарових CrN/NbN-покриттів, що складається з 270 шарів із товщиною бішару у 67 нм, під час скретч-тестування.

**Ключові слова:** багатошарові покриття, вакуумно-дугове осадження, акустична емісія, деформація, методи статистичної аналізи даних, крихкість покриття.

*(Received 27 May, 2025; in final version, 10 October, 2025)*

## 1. INTRODUCTION

The measurement of acoustic emission (AE) parameters refers to non-destructive research methods of the solid state. It is based on the registration, processing and analysis of the parameters of mechanical stress waves that occur as a result of the formation, local changes and destruction of the material structure [1–10]. The source of these waves is the local areas of the studied objects. This method is often used to research the properties of vacuum arc coatings with different architectures. The change in AE parameters of studied coatings indicates the beginning and dynamics of rapid degradation and relaxation processes in the material structure.

Acoustic emission is a phenomenon of induced spontaneous emission of acoustic waves, which is accompanied by the formation, failure, and relaxation of mechanical stresses in local volumes under the action of external fields [5]. Typical AE mechanisms are the microcracks formation [4, 7], plastic deformation [4, 11–15], phase structural transformations [16], *etc*. The excitation of acoustic waves is a certain set of physical and chemical processes occurring in the local volume of material. These processes are accompanied by a short-term release of excess energy, the elastic component of which is the external manifestation of acoustic emission [5, 10].

Some research has shown that in the load process of the vacuum arc coatings, the signal of acoustic emission appears only at the beginning of microplastic deformation, that is, it is associated with the movement of crystal lattice defects. Several works [11, 17–50] have been devoted to the research of the acoustic emission nature during deformation processes. The main acoustic emission sources are the following dislocation processes [11]: the development of slip lines [28, 29], the propagation of dislocations due to the Frank-Reed source [30, 31], dislocation exit to the free surface and dislocation annihilation [24, 32], the accelerated movement of dislocations or their movement at high speeds [33, 34], detachment of dislocation loops of critical size from their attachment sites [35, 36]. Besides that, there are other possible acoustic emission sources associated with the presence of impurities and particles of the second phase—cutting of particles by dislocations, decohesion along the interface, *etc*. [11].

The research of the acoustic emission nature during deformation processes in vacuum arc coatings with different architectures allow to obtain new data and expand the application possibilities in different fields of industry.

This paper presents the studied results of acoustic emission parameters obtained during loading of multilayer CrN/NbN coatings (bilayer thickness—67 nm, 270 layers). The influence of technological parameters of deposition on the structure formation processes of these coatings is determined.

## 2. MATERIALS AND METHODS

### 2.1. Materials and Deposition

Vacuum arc nitride multilayer CrN/NbN coatings were deposited in a modified installation 'BULAT-6'. The evaporator materials were pure metals of vacuum melting—chromium (Cr99N1) and niobium (Nb1). AISI 430 BA + PVC stainless steel samples with a mirror-polished surface were used as substrates for deposition of coatings. Surface roughness of these samples $R_a$ was lower than 0.05 μm. The dimensions of the

samples were 18×18×2 mm. They were used to determine the mechanical and tribological properties of coatings. Before deposition of the vacuum arc coatings, the vacuum chamber with the samples was pumped to a pressure of $P = 1.3 \cdot 10^{-3}$ Pa. After this, the ionic cleaning and activation of the sample surface were carried out by bombardment with metal ions at a constant voltage on it $U_S = -1.1$ kV during ten minutes. After these processes, an underlayer of pure metal was deposited to improve the adhesive properties of the coatings. The technological deposition process of multilayer nitride CrN/NbN coatings to the samples took place within 1.5 hours. The nitrogen pressure in the vacuum chamber varied from 0.08 to 0.27 Pa. The constant negative voltage on the substrate was –70 and –200 V. The arc current of evaporators was 80 A (for chromium) and 100 A (for niobium). The distance from the evaporators to the axis of substrate-holder rotation was 500 mm [51, 52].

### 2.2. Structural Characterization and Mechanical Testing

Planar raster electron microscopic images were obtained using a Tescan Vega 3 SBU in secondary electron mode at an accelerating voltage of 30 kV. The samples were examined without applying any coatings. The study of physical and mechanical characteristics of coatings on stainless steel samples was carried out by the micro-indentation method using CMS hardness measurement equipped by standard Vickers pyramid. Microhardness numbers were determined under indentation loads not higher than 1.0 N. Microtester capable for load-displacement measurements and equipped by trihedral Berkovich pyramid was used to determine Young's modulus, $E$, according to the test method procedure originally proposed by Oliver and Pharr. Scratch testing was used for research the tribological properties of multilayer CrN/NbN coatings. It was performed using scratch tester CETR-UMT (Bruker) at linearly increasing load (2–20 N) with velocity of stylus movement 0.1 mm/s during 50.08 s. The time step of measurement is 0.01 s. For these investigations was applied Rockwell diamond indenter (stylus) with 200 μm tip radius. Several parameters of testing were recorded, namely normal and tangential forces, coordinates of stylus movement, acoustic emission and friction coefficient. Total scratch length is 5 mm, total scratch depth is in range of 340–360 μm. Four scratches were carried out for each coating to increase accuracy of calculated results.

### 2.3. Calculations of Research Results

To compare the properties of multilayer CrN/NbN coatings obtained at

different deposition technological parameters, to evaluate and to determine the processes occurring during the coating deformation, methods for statistical data analysis of acoustic emission were applied. The acoustic emission of each coating was evaluated according to the following parameters: the maximum pulse amplitude $AE_{max}$, the average value $AE_{medium}$, the median $AE_{median}$, the mode $AE_{moda}$, the number of pulses $N_{AE}$ and the amplitudes sum of all acoustic emission pulses $SUM_{AE}$. The maximum value $AE_{max}$ characterizes the maximum elastic energy released when the coating is deformed. The average value $AE_{medium}$ is the mathematical expectation of a random variable, while the median $AE_{median}$ is the value located in the middle of the ranked $AE$ series. The mode $AE_{moda}$ indicates the value of the random variable that occurs most often in the set of observations. In addition, the scattering characteristics were evaluated for each of the above parameters. To increase the calculations reliability, the above parameters were evaluated for each multilayer CrN/NbN coating for four scratches.

## 3. RESULTS AND DISCUSSION

### 3.1. Parameters of Multilayer Nitride CrN/NbN Coatings and Scratches

Technological parameters of multilayer nitride CrN/NbN coatings' deposition (arc current of evaporators (chromium $I_{Cr}$ and niobium $I_{Nb}$), constant negative voltage on the substrate $U_S$, and nitrogen pressure $P_N$) and mechanical properties of these coatings (medium hardness $H_{med}$, elasticity contact modulus $E_r$, and $H_{med}/E_r$ ratio) are presented in Table 1 [51].

Table 2 shows the geometric parameters of the multilayer nitride CrN/NbN coatings, namely the layer thickness of the chromium nitride $h_{CrN}$ and niobium nitride $h_{NbN}$, the bilayer thickness $h_b$, the total thickness of the multilayer coating $h$, the number of bilayers (periods), and the total number of layers.

**TABLE 1.** Technological deposition parameters of multilayer nitride CrN/NbN coatings.

| No. sample | Coating composition | $I_{Cr}$, A | $I_{Nb}$, A | $U_S$, V | $P_N$, Pa | $H_{med}$, GPa | $E_r$, GPa | $H_{med}/E_r$ |
|---|---|---|---|---|---|---|---|---|
| 1 | CrN/NbN | 80 | 100 | –200 | 0.27 | 23.435 | 299.55 | 0.078 |
| 2 | CrN/NbN | 80 | 100 | –200 | 0.08 | 23.054 | 286.13 | 0.081 |
| 3 | CrN/NbN | 80 | 100 | –70 | 0.27 | 23.723 | 335.33 | 0.071 |
| 4 | CrN/NbN | 80 | 100 | –70 | 0.08 | 25.045 | 302.14 | 0.083 |

**TABLE 2.** Geometric parameters of multilayer nitride coatings CrN/NbN.

| Coating composition | $h_{CrN}$, nm | $h_{NbN}$, nm | $h_b$, nm | $h$, μm | Number of bilayers | Total number of layers |
|---|---|---|---|---|---|---|
| CrN/NbN | 17 | 50 | 67 | 9 | 135 | 270 |

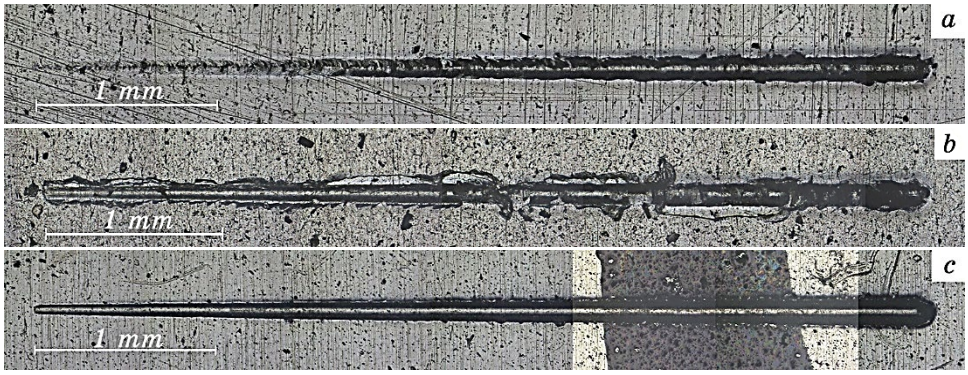


**Fig. 1.** Photographs of scratches of multilayer CrN/NbN coatings obtained at different technological parameters: $U_S = -70$ V; $P_N = 0.08$ Pa (*a*), $U_S = -70$ V; $P_N = 0.27$ Pa (*b*) and scratch of uncoated stainless steel substrate (*c*).

Since the total depth of the scratch ($h_{scratch} = 343–350$ μm) is significantly greater than the total thickness of the multilayer CrN/NbN coating ($h = 9$ μm), then for a more detailed analysis of the obtained results and separation of the substrate material influence on the calculation results, it is advisable to consider the results obtained at scratch testing in two separate stages. Namely,

1) first research stage—analysis of acoustic emission parameters obtained during time τ when $h_{scratch} = h = 9$ μm,

2) second research stage—analysis of acoustic emission data array obtained during the full time of research ($T = 50.08$ s).

Figure 1 shows scratches' photographs of multilayer CrN/NbN coatings and the uncoated stainless steel substrate.

### 3.2. Acoustic Emission Parameters of Multilayer CrN/NbN Coatings. First Research Stage

Table 3 shows the acoustic emission parameters obtained during scratch testing of uncoated stainless steel substrate (for time τ when the equation $h_{scratch} = 9$ μm is reached), namely the maximum pulse amplitude $AE_{max}$, the average value $AE_{medium}$, the median $AE_{median}$, the mode

**TABLE 3.** AE parameters of the uncoated stainless steel substrate.

| | $AE_{max}$, V | $AE_{medium}$, V | $AE_{median}$, V | $AE_{moda}$, V | $N_{AE}$ | RMSD($N_{AE}$) | $SUM_{AE}$, V | $h_{scratch}$, μm |
|---|---|---|---|---|---|---|---|---|
| Sample | 0.18 | 0.043 | 0.0417 | 0.0417 | 7 | 10.44 | 6.38 | 9 |

**TABLE 4.** AE parameters of multilayer CrN/NbN coatings.

| No. sample | $AE_{max}$, V | $AE_{medium}$, V | $AE_{median}$, V | $AE_{moda}$, V | $N_{AE}$ | RMSD($N_{AE}$) | $SUM_{AE}$, V |
|---|---|---|---|---|---|---|---|
| 1 | 1.0 | 0.069 | 0.0486 | 0.0472 | 113 | 28.28 | 24.77 |
| 2 | 0.72 | 0.081 | 0.0594 | 0.0489 | 211.33 | 12.9 | 28.48 |
| 3 | 2.18 | 0.115 | 0.0480 | 0.0471 | 92.5 | 50.43 | 41.56 |
| 4 | 0.20 | 0.061 | 0.0532 | 0.0473 | 165.67 | 8.08 | 21.44 |

$AE_{moda}$, the number of pulses $N_{AE}$, the root mean square deviation RMSD($N_{AE}$), and the sum $SUM_{AE}$.

Table 4 presents the acoustic emission parameters obtained during scratch testing of multilayer CrN/NbN coatings when the scratch depth was 9 μm. The presented parameters are based on the analysis of 4 scratches for each coating.

Figure 2 shows the dependence of the calculated acoustic emission parameters of multilayer CrN/NbN coatings and the uncoated substrate (sample) (line *3*) on constant negative voltage on the substrate (sample) $U_S$ at constant values of the nitrogen pressure $P_N$ in the vacuum chamber (line *1*—$P_N = 0.27$ Pa, line *2*—$P_N = 0.08$ Pa).

Increasing the constant negative voltage on the substrate $U_S$ from –70 to –200 V leads to:

- a decrease in the maximum value $AE_{max}$ by 2.18 times at the nitrogen pressure $P_N = 0.27$ Pa and an increase in $AE_{max}$ by 3.6 times at the nitrogen pressure $P_N = 0.08$ Pa, as can be seen in Fig. 2, *a*;
- a decrease in the average value $AE_{medium}$ by 40% at the nitrogen pressure $P_N = 0.27$ Pa and an increase in $AE_{medium}$ by 32.8% at the nitrogen pressure $P_N = 0.08$ Pa, as can be seen in Fig. 2, *b*;
- an increase in the median value $AE_{median}$ from 0.0480 V to 0.0486 V at the nitrogen pressure $P_N = 0.27$ Pa (by 1.25%, which is within calculation error) and an increase in $AE_{median}$ by 11.7% (from 0.0532 V to 0.0594 V) at the nitrogen pressure $P_N = 0.08$ Pa, as can be seen in Table 4;
- changes in the mode value $AE_{moda}$ are within 0.2% and 3.4% at the nitrogen pressure $P_N = 0.27$ Pa and 0.08 Pa, respectively, as can be seen in Table 4;
- an increase in the value $N_{AE}$ by 22.2% at the nitrogen pressure

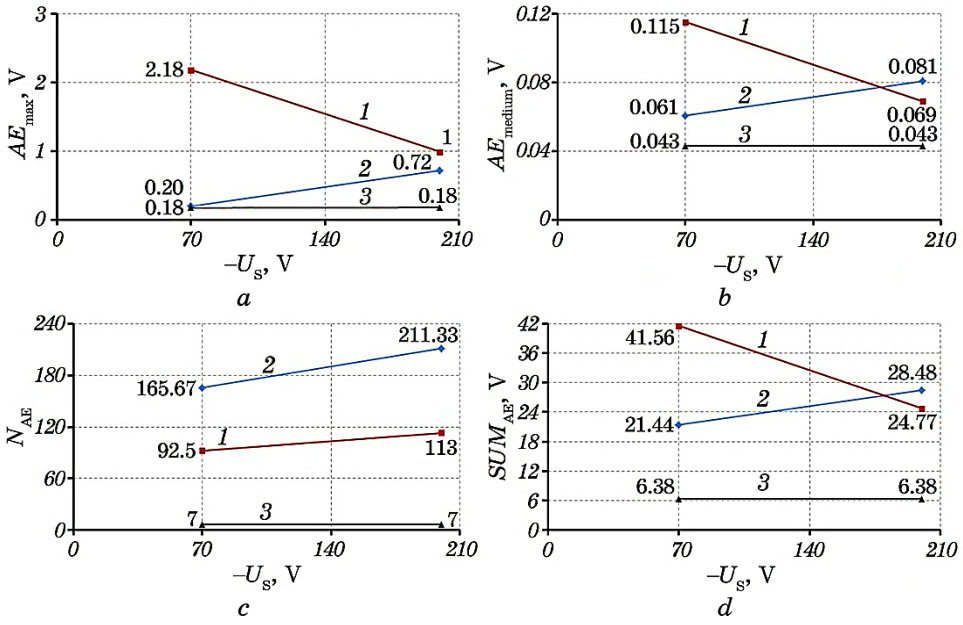


**Fig. 2.** Graphs of AE parameters' dependence of multilayer CrN/NbN coatings and the substrate on the deposition technological parameter $U_S$ at constant values of the nitrogen pressure in the vacuum chamber $P_N$: $AE_{max}$ (*a*); $AE_{medium}$ (*b*); $N_{AE}$ (*c*); $SUM_{AE}$ (*d*).

$P_N = 0.27$ Pa, as can be seen in Fig. 2, *c*. At the same time root mean square deviation RMSD($N_{AE}$) decreases by 1.8 times (from 50.43 to 28.28), as can be seen in Table 4;

• an increase in the value $N_{AE}$ by 27.6% at the nitrogen pressure $P_N = 0.08$ Pa, as can be seen in Fig. 2, *c*, and root mean square deviation RMSD($N_{AE}$) increases by 1.6 times (from 8.08 to 12.9), as can be seen in Table 4;

• a decrease in the value $SUM_{AE}$ by 40.4% at the nitrogen pressure $P_N = 0.27$ Pa and an increase in $SUM_{AE}$ by 32.8% at the nitrogen pressure $P_N = 0.08$ Pa, as can be seen in Fig. 2, *d*.

Figure 3 shows the dependence of the calculated acoustic emission parameters of multilayer CrN/NbN coatings and the uncoated substrate (line *3*) on the nitrogen pressure $P_N$ at constant negative voltage on the substrate $U_S$ (line *1*—$U_S = -70$ V, line *2*—$U_S = -200$ V).

Increasing in the nitrogen pressure $P_N$ in the vacuum chamber from 0.08 to 0.27 Pa leads to:

• an increase in the maximum value $AE_{max}$ by 10.9 and 1.4 times at the constant negative voltage on the substrate $U_S = -70$ V and –200 V, respectively, as can be seen in Fig. 3, *a*;

• an increase in the average value $AE_{medium}$ by 88.5% at the constant

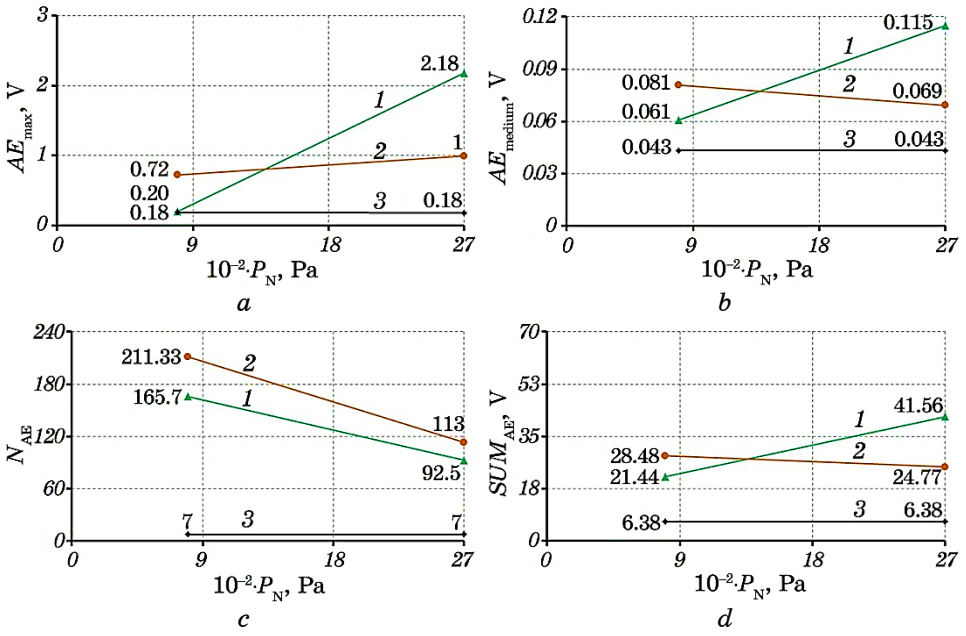


**Fig. 3.** Graphs of AE parameters' dependence of multilayer CrN/NbN coatings and substrate on the deposition technological parameter $P_N$ at the constant negative voltage on the substrate $U_S$: $AE_{max}$ (*a*); $AE_{medium}$ (*b*); $N_{AE}$ (*c*); $SUM_{AE}$ (*d*).

negative voltage on the substrate $U_S = -70$ V and a decrease in $AE_{medium}$ by 14.8% at the constant negative voltage on the substrate $U_S = -200$ V, as can be seen in Fig. 3, *b*;

• a decrease in the median value $AE_{median}$ by 9.8% (from 0.0532 V to 0.0480 V) and 18.2% (from 0.0594 V to 0.0486 V) at the constant negative voltage on the substrate $U_S = -70$ V and –200 V, respectively, as can be seen in Table 4;

• a decrease in the mode value $AE_{moda}$ by 0.42% and 3.5% at the constant negative voltage on the substrate $U_S = -70$ V and –200 V, respectively, as can be seen in Table 4;

• a decrease in the value $N_{AE}$ by 44.2% and 46.5% at the constant negative voltage on the substrate $U_S = -70$ V and –200 V, respectively, as can be seen in Fig. 3, *c*;

• an increase in the value $SUM_{AE}$ by 93.8% at the constant negative voltage on the substrate $U_S = -70$ V and a decrease in the value $SUM_{AE}$ by 13% at the constant negative voltage on the substrate $U_S = -200$ V, as can be seen in Fig. 3, *d*.

The graphs of dependence in Figs. 2, 3 show the structure reconstruction of the multilayer CrN/NbN coatings. It is accompanied by

the formation, breakdown and relaxation of mechanical stresses in local volumes of the coatings under the load ($F = 2.8$ H). Obtained results show structural heterogeneity within the volume of multilayer CrN/NbN coatings and indicate the presence of local microvolumes in the coating with a greater number of defects (dislocations, vacancies, *etc.*). The multilayer structure of CrN/NbN coatings (270 layers with layer thicknesses $h_{CrN} = 17$ nm, $h_{NbN} = 50$ nm) also affects the studied parameters.

### 3.3. Acoustic Emission Parameters of Multilayer CrN/NbN Coatings. Second Research Stage

Table 5 shows the acoustic emission parameters obtained during scratch testing of the uncoated stainless steel sample over the full research time ($T = 50.08$ s), namely, the maximum pulse amplitude $AE_{max}$, the average value $AE_{medium}$, the median $AE_{median}$, the mode $AE_{moda}$, the number of pulses $N_{AE}$, the root mean square deviation RMSD($N_{AE}$), the sum of amplitudes of all acoustic emission pulses $SUM_{AE}$, and the scratch depth $h_{scratch}$.

Table 6 presents the acoustic emission parameters obtained during scratch testing of multilayer CrN/NbN coatings for the full time of research ($T = 50.08$ s). These parameters are based on the analysis of 4 scratches for each coating.

Figure 4 shows the dependences of the calculated acoustic emission parameters of multilayer CrN/NbN coatings and the uncoated substrate (line *3*) on the constant negative voltage on the substrate (sample) $U_S$ at constant values of the nitrogen pressure $P_N$ in the vacuum

**TABLE 5.** AE parameters of the uncoated stainless steel substrate.

| | $AE_{max}$, V | $AE_{medium}$, V | $AE_{median}$, V | $AE_{moda}$, V | $N_{AE}$ | RMSD($N_{AE}$) | $SUM_{AE}$, V | $h_{scratch}$, μm |
|---|---|---|---|---|---|---|---|---|
| Sample | 8.5 | 0.252 | 0.0615 | 0.0414 | 1079 | 88.3 | 506 | 347.3 |

**TABLE 6.** AE parameters of multilayer CrN/NbN coatings.

| No. sample | $AE_{max}$, V | $AE_{medium}$, V | $AE_{median}$, V | $AE_{moda}$, V | $N_{AE}$ | RMSD($N_{AE}$) | $SUM_{AE}$, V | $h_{scratch}$, μm |
|---|---|---|---|---|---|---|---|---|
| 1 | 1.76 | 0.084 | 0.0649 | 0.0478 | 3729 | 30 | 422 | 348.1 |
| 2 | 8.99 | 0.374 | 0.0919 | 0.0544 | 4394 | 115 | 1872 | 344 |
| 3 | 6.89 | 0.196 | 0.0613 | 0.0480 | 3077 | 294 | 982 | 349.3 |
| 4 | 6.77 | 0.143 | 0.0859 | 0.0600 | 4544 | 55 | 716 | 342.3 |

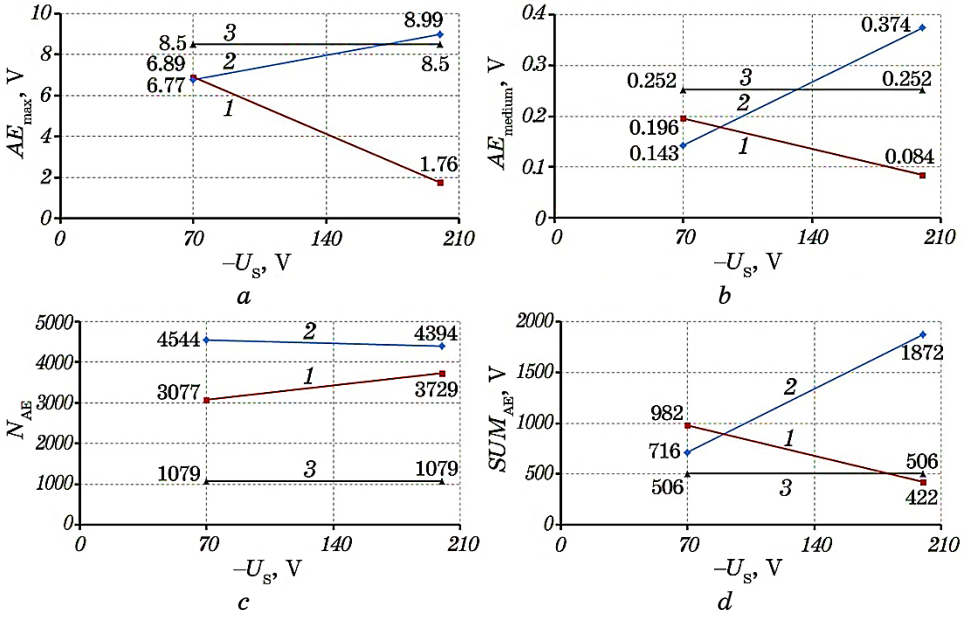


**Fig. 4.** Graphs of acoustic emission parameters' dependence of multilayer CrN/NbN coatings and the substrate on the deposition technological parameter $U_S$ at constant values of the nitrogen pressure in the vacuum chamber $P_N$: $AE_{max}$ (*a*); $AE_{medium}$ (*b*); $N_{AE}$ (*c*); $SUM_{AE}$ (*d*).

chamber (line *1*—$P_N = 0.27$ Pa, line *2*—$P_N = 0.08$ Pa).

Increasing the constant negative voltage on the substrate $U_S$ from –70 to –200 V leads to:

- a decrease in the maximum value $AE_{max}$ by 74.5% at the nitrogen pressure $P_N = 0.27$ Pa and an increase in $AE_{max}$ by 32.8% at the nitrogen pressure $P_N = 0.08$ Pa, as can be seen in Fig. 4, *a*;
- a decrease in the average value $AE_{medium}$ by 57% at the nitrogen pressure $P_N = 0.27$ Pa and an increase in $AE_{medium}$ by 161.5% at the nitrogen pressure $P_N = 0.08$ Pa, as can be seen in Fig. 4, *b*;
- an increase in the median value $AE_{median}$ by 6% and 7% at the nitrogen pressure $P_N = 0.27$ Pa and 0.08 Pa, respectively, as can be seen in Table 6;
- a decrease in the mode value $AE_{moda}$ by 0.4% and 9.3% at the nitrogen pressure $P_N = 0.27$ Pa and 0.08 Pa, respectively, as can be seen in Table 6;
- an increase in the value $N_{AE}$ by 21.2% at the nitrogen pressure $P_N = 0.27$ Pa and a decrease in $N_{AE}$ by 3.3% at the nitrogen pressure $P_N = 0.08$ Pa, as can be seen in Fig. 4, *c*;
- a decrease in the value RMSD($N_{AE}$) by 10 times at the nitrogen pressure $P_N = 0.27$ Pa and an increase in RMSD($N_{AE}$) by 2 times at the

nitrogen pressure $P_N = 0.08$ Pa, as can be seen in Table 6;

- a decrease in the value $SUM_{AE}$ by 57% at the nitrogen pressure $P_N = 0.27$ Pa and an increase in $SUM_{AE}$ by 161.5% at the nitrogen pressure $P_N = 0.08$ Pa, as can be seen in Fig. 4, *d*.

Figure 5 shows the dependence of the calculated acoustic emission parameters of multilayer CrN/NbN coatings and the substrate (line *3*) on the nitrogen pressure $P_N$ at constant negative voltage on the substrate $U_S$ (line *1*—$U_S = -70$ V, line *2*—$U_S = -200$ V).

Increasing in the nitrogen pressure $P_N$ in the vacuum chamber from 0.08 to 0.27 Pa leads to:

- an increase in the maximum value $AE_{max}$ by 1.8% at the constant negative voltage on the substrate $U_S = -70$ V and a decrease in $AE_{max}$ by 80.4% at the voltage $U_S = -200$ V, as can be seen in Fig. 5, *a*;

- an increase in the average value $AE_{medium}$ by 37% at the constant negative voltage on the substrate $U_S = -70$ V and a decrease in $AE_{medium}$ by 77.5% at the voltage $U_S = -200$ V, as can be seen in Fig. 5, *b*;

- a decrease in the median value $AE_{median}$ by 28.6% and 29.4% at the constant negative voltage on the substrate $U_S = -70$ V and −200 V, respectively, as can be seen in Table 6;

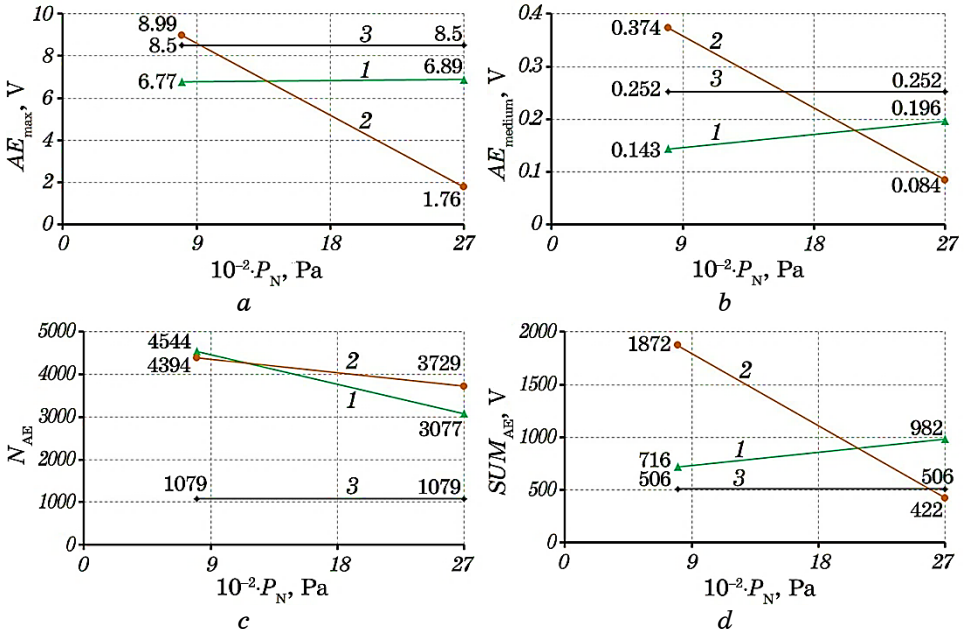


**Fig. 5.** Graphs of acoustic emission parameters' dependence of multilayer CrN/NbN coatings and the substrate on the deposition technological parameter $P_N$ at the constant negative voltage on the substrate $U_S$: $AE_{max}$ (*a*); $AE_{medium}$ (*b*); $N_{AE}$ (*c*); $SUM_{AE}$ (*d*).

- a decrease in the mode value $AE_{moda}$ by 20% and 12% at the constant negative voltage on the substrate $U_S = -70$ V and $-200$ V, respectively, as can be seen in Table 6;
- a decrease in the value $N_{AE}$ by 32.3% and 15% at the constant negative voltage on the substrate $U_S = -70$ V and $-200$ V, respectively, as can be seen in Fig. 5, *c*;
- an increase in the value RMSD($N_{AE}$) by 5.3 times at the constant negative voltage on the substrate $U_S = -70$ V and a decrease in RMSD($N_{AE}$) by 3.8 times at the voltage $U_S = -200$ V, as can be seen in Table 6;
- an increase in the value $SUM_{AE}$ by 37% at the constant negative voltage on the substrate $U_S = -70$ V and a decrease in $SUM_{AE}$ by 77.5% at the voltage $U_S = -200$ V, as can be seen in Fig. 5, *d*.

The graphs in Figures 4–5 clearly demonstrate the local structure reconstruction of the multilayer CrN/NbN coating together with the substrate, which is accompanied by the formation, breakdown and relaxation of mechanical stresses in local volumes of not only the coating, but also the substrate under the action of a higher load ($F = 20$ N).

The analysis of *AE* parameters at this research stage showed that the nitrogen pressure $P_N$ affects the parameter $AE_{moda}$ the most. The increase in $P_N$ leads to a decrease in $AE_{moda}$.

Figure 6 shows the acoustic emission amplitude *AE* observed when a substrate with the multilayer CrN/NbN coatings (sample No. 4—technological parameters of deposition $U_S = -70$ V and $P_N = 0.08$ Pa, and sample No. 3—technological parameters of deposition $U_S = -70$ V and $P_N = 0.27$ Pa) and uncoated substrate are scratched. The load *F* was changing from 2 to 20 N.

The amplitude and shape of the acoustic emission peaks are affected not only by the physical and chemical properties of the coating components (CrN and NbN), but also by the multilayer coatings' architecture (the number of layers and their thicknesses, properties of the interlayer boundary, *etc.*).

## 4. CONCLUSION

The dependence of the acoustic emission parameters on the deposition technological parameters (constant negative voltage on the substrate $U_S$, nitrogen pressure $P_N$) was investigated. This study characterizes the multilayer CrN/NbN coating with 270 layers (135 bilayers), bilayer thickness $h_b = 67$ nm.

The obtained research results can be summarized in the form of the following conclusions:

1. The change trend of the parameter $AE_{max}$ remains unchanged at increasing in the constant negative voltage both at the beginning of the scratch and along its entire scratch length. But increasing the nitrogen pressure in the vacuum chamber at the constant negative voltage

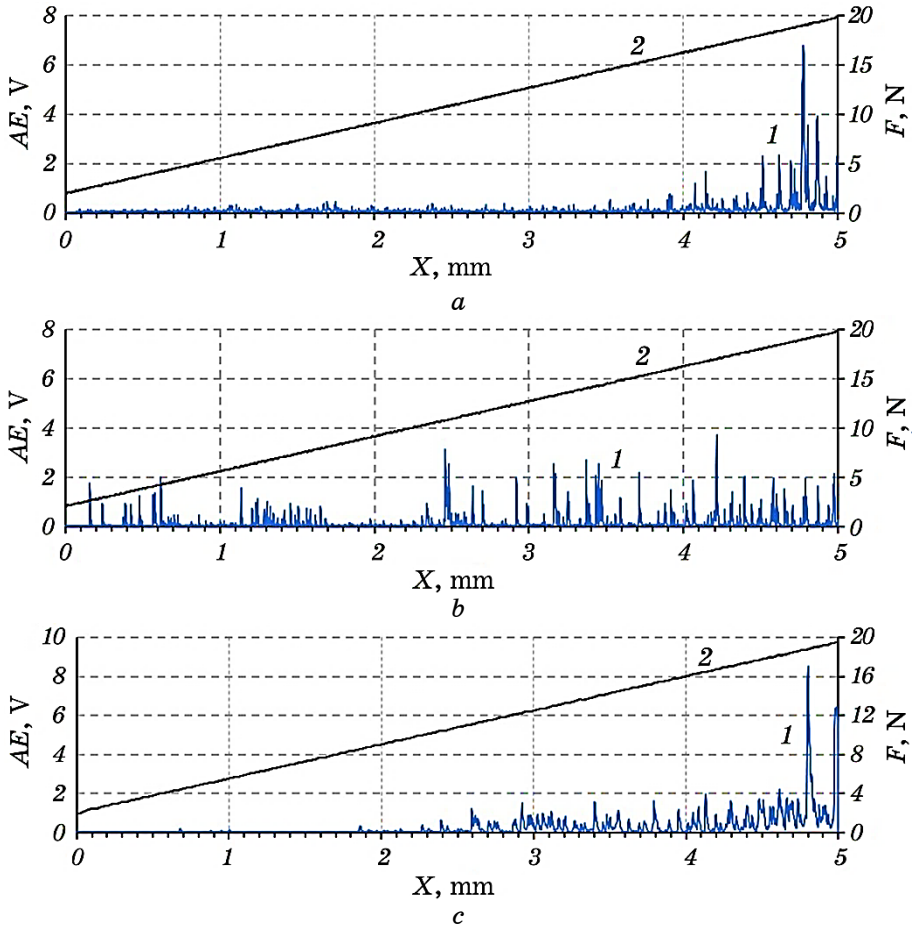


**Fig. 6.** Dependence of the acoustic emission AE of multilayer CrN/NbN coatings and substrate on the movement of diamond indenter (stylus): sample No. 4 (*a*), sample No. 3 (*b*), uncoated substrate (*c*) at the load *F*.

$U_S = -200$ V leads to changing this trend from increasing in $AE_{max}$ by 39% at the beginning of the scratch to decreasing in $AE_{max}$ by 80.4% along scratch length.

2. The change trend of the parameter $AE_{medium}$ remains unchanged both at the beginning of the scratch and along its entire scratch length. These changes are more significant along the entire scratch length, except in case of increasing in the nitrogen pressure at the voltage on the substrate $U_S = -70$ V, when $AE_{medium}$ increases by 88.5% at the beginning of the scratch.

3. The change trend of the parameter $AE_{median}$, which characterises the median value by position, remains unchanged both at the beginning of

the scratch and along its entire length, depending on the technological parameter ($U_S$, $P_N$) of the coating deposition. The change range of the parameter $AE_{median}$ is from 1.25% to 18.2% at the beginning of the scratch and from 6% to 29.4% along the entire length of the scratch.

4. The change trend of the parameter $N_{AE}$ depending on the technological parameter of coating deposition remains unchanged both at the beginning of the scratch and along the entire length of the scratch, except in case of increasing in the constant negative voltage $U_S$ at the nitrogen pressure in vacuum chamber $P_N = 0.08$ Pa, when $N_{AE}$ increases by 27.6% at the beginning of the scratch and decreases by 3.3% along the entire scratch length.

5. Along the entire scratch length, parameters $AE_{medium}$ and $SUM_{AE}$ have the same trend of changes, unlike the parameter $N_{AE}$.

The obtained research results can help us understand the changes in the coating structure under loading along the entire scratch length. It can be used for prediction of the multilayer coatings' properties depending on the technological parameters of the deposition and the coating architecture.

## REFERENCES


1. A. E. Lord and W. Mason, *Phys. Acoustic*, **11**: 289 (1975).
2. M. V. Kravtsov, O. V. Lyashenko, and A. P. Onanko, *Funct. Mater.*, **11**, No. 2: 353 (2004).
3. O. V. Lyashenko and V. P. Veleshchuk, *Ukr. J. Phys.*, **48**, No. 9: 981 (2003) (in Ukrainian).
4. O. V. Gusev, *Akusticheskaya Emissiya pri Deformatsii Monokristallov Tugoplavkikh Metallov* [Acoustic Emission During Deformation of Single Crystals of Refractory Metals] (Moskva: Nauka: 1982).
5. O. I. Vlasenko, M. P. Kyseliuk, V. P. Veleshchuk, Z. K. Vlasenko, I. O. Lyashenko, and O. V. Lyashenko, *Optoelectronics and Semiconductor Technique*, **49**: 5 (2014) (in Ukrainian).
6. V. M. Perga, *Novi Metody Doslidzhennya Fizychnykh Vlastyvostei Tverdykh Til. Akustychna Emisiya. Chastyny 1 i 2* [New Methods of Studying the Physical Properties of Solid Bodies. Acoustic Emission. Parts 1 and 2] (Kyiv: 1991).
7. V. P. Babak and S. F. Filonenko, *Advances in Aerospace Technology*, **1**, No. 1: 54 (1998) (in Ukrainian).
8. V. I. Artiukhov, K. B. Vakar, and V. I. Makarov, *Akusticheskaya Emissiya i Yeyo Primenenie dlya Nerazrushayushchego Kontrolya v Yadernoi Ehnergetike* [Acoustic Emission and its Application for Non-Destructive Testing in Nuclear] (Moskva: Atomizdat: 1980).
9. V. A. Kalitenko, V. M. Perga, and I. N. Salivonov, *Phys. Solid State*, **22**, No. 6: 1838 (1980).
10. DSTU 2374-94, *Rozrakhunky na Mitsnist ta Vyprobuvannya Tekhnichnykh Vyrobiv. Akustychna Emisiya* [Strength Calculations and Testing of Technical Products. Acoustic Emission] (Kyiv: Derzhstandart Ukrainy: 1994) (in Ukrainian).

11. A. Yu. Vinogradov and D. L. Merson, *Low Temp. Phys.*, **44**, No. 9: 1186 (2018).
12. A. M. Leskovskyi and Sh. Sh. Azimov, *Tech. Phys. Lett.*, **10**, No. 5: 307 (1997).
13. G. I. Prokopenko, T. V. Golub, O. N. Kashevskaia, B. N. Mordyuk, N. A. Efymov, and V. G. Bezkorovainyi, *Metallofiz. Noveishie Tekhnol.*, **28**, No. 2: 151 (2006).
14. L. V. Tikhonov and G. I. Prokopenko, *Tech. Diagnostics and Non-Destructive Testing*, **8**: 73 (1991).
15. P. I. Stoev, I. I. Papirov, and V. I. Moschenok, *Probl. Atom. Sci. Tech.*, **1**: 15 (2006).
16. V. A. Kalitenko, I. Ya. Kucherov, V. M. Perga, and V. A. Tkhoryk, *Phys. Solid State*, **30**, No. 12: 3677 (1988).
17. B. Polyzos, E. Douka, and A. Trochidis, *J. Appl. Phys.*, **89**: 2124 (2001).
18. A. Sendrowicz, A. O. Myhre, A. V. Danyuk, and A. Vinogradov, *Mater. Sci. Eng. A*, **856**: 143969 (2022).
19. A. M. Kosevich and V. S. Boyko, *Physics-Uspekhi*, **104**: 201 (1971).
20. A. M. Kosevich, *Ukr. J. Phys.*, **84**: 579 (1964).
21. J. D. Eshelby, *Proc. Roy. Soc.*, **260**: 222 (1962).
22. A. Trochidis and B. Polyzos, *J. Mech. Phys. Solids*, **42**: 1933 (1994).
23. D. G. Eitzen and H. N. G. Wadley, *J. Res. Natl. Bur. Stand.*, **89**: 75 (1984).
24. N. Kiesewetter and P. Schiller, *Scr. Met.*, **8**: 249 (1974).
25. A. Trochidis and B. Polyzos, *J. Appl. Phys.*, **78**: 170 (1995).
26. A. M. Kosevich, *Zh. Eksp. Teor. Fiz*, **42**: 152 (1962).
27. V. R. Skalskyi, Yu. Ya. Matviiv, and O. G. Simakovych, *Physicochemical Mechanicals of Materials*, **48**, No. 6: 76 (2012).
28. Yu. B. Drobot and V. V. Korchevsky, *Flaw Detection*, **6**: 38 (1985).
29. R. M. Fisher and L. S. Lally, *Canad. J. Phys.*, **45**: 1147 (1967).
30. J. R. Frederick and D. K. Felbeck, *Acoustic Emission* (Baltimore: ASTM STP: 1972).
31. T. Imanaka and K. Sano, *Crystal Lattice Defects*, **4**: 57 (1973).
32. V. S. Boyko, V. F. Kivshik, and L. F. Krivenko, *Zh. Eksp. Teor. Fiz*, **78**: 797 (1980).
33. C. B. Scruby and H. N. G. Wadley, *Met. Science*, **15**: 599 (1981).
34. D. Rouby and P. Fleischmann, *Internal Friction and Ultrasonic Attenuation Solids* (1977), p. 811.
35. D. R. James and S. N. Carpenter, *J. Appl. Phys.*, **42**: 4685 (1971).
36. F. P. Higgins and S. N. Carpenter, *Acta Metallurg.*, **26**: 133 (1978).
37. N. H. Faisal, R. Ahmed, and R. L. Reuben, *Int. Mat. Rev.*, **56**, No. 2: 98 (2011).
38. S. Yamamoto and H. Ichimura, *J. Mater. Res.*, **7**: 2240 (1992).
39. R. K. Choudhary and P. Mishra, *J. of Mater. Eng. and Perform.*, **25**: 2454 (2016).
40. M. A. Hassan, A. R. Bushroa, and Reza Mahmoodian, *Surf. Coat. Tech.*, **277**: 216 (2015).
41. Kaoru Ikenaga, Akira Yanagida, and Akira Azushima, *J. of Solid Mechanics and Materials Engineering*, **3**, No. 2: 347 (2009).
42. J. Tomastik, R. Ctvrtlik, P. Bohac, M. Drab, V. Koula, K. Cvrk, and L. Jastrabik, *Key Eng. Mater.*, **662**: 119 (2015).
43. B. Warcholiński, A. Gilewicz, Z. Kukliński, and P. Myśliński, *Vacuum*, **83**, No. 4: 715 (2008).
44. Nicholas X. Randall, *Surf. Coat. Tech.*, **380**: 125092 (2019).

45. J. Tomastik, R. Ctvrtlik, M. Drab, and J. Manak, *Coatings*, **8**, No. 5: 196 (2018).
46. E. Hamzah, M. Ali, and M. R. HJ. Mohd Toff, *Surf. Rev. Lett.*, **13**, No. 6: 763 (2006).
47. H. Jensen, U. M. Jensen, and G. Sorensen, *Surf. Coat. Tech.*, **74–75**: 297 (1995).
48. P. Drobný, D. Mercier, V. Koula, S. I. Škrobáková, L. Čaplovič, and M. Sahul, *Coatings*, **11**, No. 8: 919 (2021).
49. Tian-Shun Dong, Ran Wang, Guo-Lu Li, and Liu Ming, *High Temp. Mater. Proc.*, **38**: 601 (2019).
50. T. Z. Kattamis, F. Chang, and M. Levy, *Surf. Coat. Tech.*, **43–44**, No. 1: 390 (1990).
51. I. V. Serdiuk, S. I. Petrushenko, V. O. Stolbovyi, and M. Fijalkowski, *Metallofiz. Noveishie Tekhnol.*, **46**, No. 1: 23 (2024).
52. V. P. Rudenko, V. O. Stolbovoy, I. V. Serdiuk, and K. G. Kartmazov, *East.-Eur. J. Enterp. Tech.*, **48**, No. 6/1: 66 (2010).